

MICROCOPY RESOLUTION TEST CHART  
NATIONAL BUREAU OF STANDARDS-1963-A

AFOSR-TR-83-0143

2



Department of AERONAUTICS and ASTRONAUTICS  
STANFORD UNIVERSITY

Report AA CFD 83-1

ADA 126508

FIRST ANNUAL SCIENTIFIC REPORT

January 1, 1982 to December 31, 1982

Air Force Office of Scientific Research Contract AFOSR-82-0083

COHERENT STRUCTURE MODELING OF VISCOUS SUBLAYER TURBULENCE  
FOR INCOMPRESSIBLE FLOW WITH HEAT TRANSFER  
AND FOR COMPRESSIBLE FLOW

BY

DALE K. OTA AND DEAN R. CHAPMAN

Submitted to the

Directorate of Aerospace Sciences  
Air Force Office of Scientific Research  
Bolling AFB  
Washington D.C. 20332

by the

Department of Aeronautics and Astronautics  
Stanford University  
Stanford, CA 94305-2186

DTIC FILE COPY

Approved for public release;  
distribution unlimited.

February 1983

DTIC  
ELECTE  
APR 06 1983  
S E D

88 04 05 157

**UNCLASSIFIED**

SECURITY CLASSIFICATION OF THIS PAGE (When Data Entered)

REPORT DOCUMENTATION PAGE		READ INSTRUCTIONS BEFORE COMPLETING FORM
1. REPORT NUMBER <b>AFOSR-TR- 83-0143</b>	2. GOVT ACCESSION NO. <b>ADA126506</b>	3. RECIPIENT'S CATALOG NUMBER
4. TITLE (and Subtitle) <b>Coherent Structure Modeling of Viscous Sublayer Turbulence for Incompressible Flow with Heat Transfer and for Compressible Flow</b>		5. TYPE OF REPORT & PERIOD COVERED <b>First Annual Scientific Report Jan. 1, 1982 to Dec. 31, 1982</b>
7. AUTHOR(s) <b>Dale K. Ota and Dean R. Chapman</b>		6. PERFORMING ORG. REPORT NUMBER
9. PERFORMING ORGANIZATION NAME AND ADDRESS <b>Department of Aeronautics and Astronautics Stanford University Stanford, CA 94305</b>		8. CONTRACT OR GRANT NUMBER(s) <b>AFOSR-82-0083</b>
11. CONTROLLING OFFICE NAME AND ADDRESS <b>Directorate of Aerospace Sciences Air Force Office of Scientific Research Bolling AFB, Washington D.C. 20332</b>		10. PROGRAM ELEMENT, PROJECT, TASK AREA & WORK UNIT NUMBERS <b>61102F 2307/K1</b>
14. MONITORING AGENCY NAME & ADDRESS (if different from Controlling Office)		12. REPORT DATE <b>Feb 1983</b>
		13. NUMBER OF PAGES <b>33</b>
		15. SECURITY CLASS. (of this report) <b>Unclassified</b>
		15a. DECLASSIFICATION/DOWNGRADING SCHEDULE
16. DISTRIBUTION STATEMENT (of this Report)  <b>Approved for public release; distribution unlimited.</b>		
17. DISTRIBUTION STATEMENT (of the abstract entered in Block 20, if different from Report)		
18. SUPPLEMENTARY NOTES		
19. KEY WORDS (Continue on reverse side if necessary and identify by block number) <b>Fluid Mechanics, heat transfer, turbulent Prandtl number, viscous sublayer, Navier-Stokes, Computational Model</b>		
20. ABSTRACT (Continue on reverse side if necessary and identify by block number) <b>The general objective of the present research is to develop a Navier-Stokes computational model of the time-dependent dynamics and heat transfer in a compressible viscous sublayer. Specific objectives are to compute the variation of turbulent Prandtl number across the sublayer for fluids of different molecular Prandtl number, and for flows with streamwise pressure gradient.</b> → <b>...over</b>		

DD FORM 1473  
1 JAN 73

**UNCLASSIFIED**

SECURITY CLASSIFICATION OF THIS PAGE (When Data Entered)

UNCLASSIFIED

SECURITY CLASSIFICATION OF THIS PAGE(When Data Entered)

20. cont'd.

Various existing theories for turbulent Prandtl number near a wall are shown to differ greatly. An exact analytical solution for oscillating shear flow with heat transfer has been derived and used to test satisfactorily the accuracy of the numerical algorithms to be used in the equations of motion for the time-dependent, heat-conduction, and viscous terms. Most of the necessary programming to adapt the Pulliam-Steger code to viscous sublayer modeling has been completed, and some debugging has begun. Boundary conditions have been formulated for the first test case without heat transfer, and for the initial runs to be made with heat transfer.

Accession For	
NTIS GRA&I	<input checked="" type="checkbox"/>
DTIC TAB	<input type="checkbox"/>
Unannounced	<input type="checkbox"/>
Justification	
By _____	
Distribution/	
Availability Codes	
Dist	Avail and/or Special
A	



UNCLASSIFIED

SECURITY CLASSIFICATION OF THIS PAGE(When Data Entered)

## INTRODUCTION AND OBJECTIVES

Practical applications of computational fluid dynamics within the foreseeable future must necessarily utilize some form of turbulence modeling. Computations based on the Reynolds-averaged equations of motion require all turbulence transport of momentum and energy to be modeled; while large-eddy simulations require the subgrid-scale turbulence to be modeled. In both cases, the uncertainties in modeling turbulence within the viscous sublayer constitute a major weak link in the overall numerical computation.

During the past two decades a great deal of new experimental information has been assembled on the physics of organized eddy structures in turbulent flow, especially within the viscous sublayer (see, for example, the recent review of Cantwell, 1981). Yet it has not been possible thus far to incorporate this body of physical information within the framework of Reynolds-averaged turbulence modeling. The reason is fundamental, reflecting a well-known limitation in the Reynolds-average approach which begins by time averaging the dynamic equations of motion. In this initial mathematical step important physical aspects of organized eddy structures, such as phase relationships and coherent structure dynamics, are obliterated irreversibly. Consequently, some totally different approach is required if the observed physics of coherent eddy motions are to be incorporated within the framework of a turbulence model.

Quite recently a new approach has been developed for modeling viscous sublayer turbulence in incompressible flow without heat transfer (Chapman and Kuhn (1981). Their method models directly the essential organized eddy structures observed in experiments. The principal steps in this "coherent-structure modelling" are: first, to model velocity boundary conditions at the outer edge of the viscous sublayer, then to compute time-dependent dynamics, and finally to time average com-

puted results. Thus, time averaging is the last operation performed on computed dynamics, rather than the first operation performed on the dynamic equations. This initial effort, although far from fully developed, already has been surprisingly successful in modeling some important characteristics of viscous sublayer turbulence.

The over all objective of the present research is to develop, using the Navier-Stokes equations, a computational model of viscous sublayer turbulence applicable to flow with heat transfer and to compressible flow. Specific tasks within this objective are to utilize the model to compute the distribution of turbulent Prandtl number within the viscous sublayer (a) for fluids of various molecular Prandtl number, and (b) for flows with adverse, zero, and favorable streamwise pressure gradients.

Navier-Stokes computations of the turbulent Prandtl number  $Pr_t$  are significant because experimental techniques have been unable to provide reliable measurements within the viscous sublayer. This parameter, of course, affects turbulent heat transfer. Since by definition,

$$Pr_t = \frac{(\overline{uv}) \left( \frac{\partial \bar{\theta}}{\partial y} \right)}{(\overline{\theta v}) \left( \frac{\partial \bar{U}}{\partial y} \right)}$$

an experimental determination would require accurate measurements near a wall of the Reynolds stress  $\overline{uv}$ , the correlation  $\overline{\theta v}$  between temperature  $\theta$  and normal velocity, the mean velocity gradient  $\partial \bar{U} / \partial y$ , and the mean temperature gradient  $\partial \bar{\theta} / \partial y$ . To date, it has not been possible to make reliable measurements of these four quantities in the viscous sublayer. The band of uncertainty from one set of data for air (Simpson et al. (1970)), is illustrated in fig. 1. Other sets of experimental data, e.g. Fulachier (1972), indicate that the overall uncertainty band is even broader than this one set of measurements would indicate. Experiments are unable to determine whether the values of  $Pr_t$  near a wall are large, small, or intermediate. Experiments

also have not been able to define how  $Pr_t$  varies with molecular  $Pr$  or with pressure gradient. We believe that Navier-Stokes computations can shed much light on these uncertainties.

## MOTIVATIONS FOR COHERENT STRUCTURE MODELING OF VISCOUS SUBLAYER TURBULENCE

Coherent-structure modeling departs markedly from Reynolds-averaging modeling, and thereby offers the potential of some entirely new advances in turbulence computation. Both the motivations and the payoff for this type of research are quite different from those for more conventional turbulence modeling. In addition to the specific motivations outlined above for the objectives of the present research, there are other important motivations that will affect different areas of turbulence computation. It is appropriate, therefore, to outline some of these.

Three other motivations for developing a realistic coherent-structure model of viscous sublayer turbulence are:

1. - *To Strengthen a major weak link in present Reynolds-Average closure Schemes.* Conventional turbulence closure methods (e.g.  $k-\epsilon$ , other 2-equation methods, and Reynolds-Stress transport methods) all employ differential transport equations that are "modeled" forms of exact transport equations. The exact equation for the transport of dissipation, for example, contains very complex turbulence terms involving pressure-velocity correlations, triple correlations of velocity gradients, correlations of second derivatives of velocity, and correlations between pressure gradient and velocity gradient. Such correlations are not measurable with present experimental technology. Because modeled equations for free turbulence yield demonstrably incorrect results near a wall, various *ad hoc* functions (up to 5 in number) are added in an effort to mend this shortcom-

ing. Without any guide or test basis from experiment, the inevitable consequence is that different models with different ad hoc functions yield different results for technically important quantities such as skin friction in flows with pressure gradient (Patel et. al 1981). If, however, a *realistic* Navier-Stokes computational model were developed for the time dependent dynamics of viscous sublayer flow, then all the terms in the exact transport equations could be computed. When compared with corresponding modeled terms, a rational formulation would be obtained of the wall damping functions for integrating turbulence models across the viscous sublayer. This would strengthen a major weak link in conventional turbulence models. Reynolds-average modeling, of course, will be the mainstay of practical turbulent flow computation for years to come.

2. - *To provide a simple test flow against which subgrid scale models of turbulence in large eddy simulations can be tested.* The simple flow of homogeneous shear, for example, computed in detail from the time-dependent Navier-Stokes equations (Rogallo 1977) has been used effectively as a test flow for assessing subgrid scale turbulence models for application in the outer region of a turbulent boundary layer or in free shear layers (e.g., Clark et. al. 1979, McMillan and Ferziger 1979, Shirani 1981). A realistic coherent-structure model of viscous sublayer turbulence, likewise computed from the time-dependent Navier-Stokes equations, could similarly be used to test subgrid-scale models for large eddy simulations of turbulent flow in the region adjacent to a wall.
  
3. - *To provide a guide for modeling the lower boundary conditions for the outer turbulent region in large eddy simulations of boundary layer flow.* If a realistic boundary condition of this type could be developed, the entire viscous sublayer could be modeled rather than directly computed. The required computer power

for large eddy simulations at high Reynolds numbers would thereby be reduced by a very large factor (about  $10^3$ ; Chapman, 1980).

In summary of the motivations for developing coherent-structure turbulence models, it is clear that the potential payoffs are significant and of much broader scope than the specific objectives of the present research. Benefits are anticipated to conventional Reynolds-average models of near-term application, as well as to future large eddy simulation models of longer range application.

## FORMULATION OF COMPUTATIONAL MODEL

### Differential Equations

The numerical scheme selected to solve the Navier-Stokes equations is an adaptation of the Pulliam and Steger (1980) code for compressible flow. Velocities in the physical  $x, \bar{y}, \bar{z}$  domain are  $u, \bar{v}, \bar{w}$ . In the computational  $\xi, \eta, \zeta$ , domain the dependent variables are  $\rho, \rho u, \rho \bar{v}, \rho \bar{w}$ , and  $\rho[e_i + (u^2 + \bar{v}^2 + \bar{w}^2)/2]$ , where  $e_i$  is the internal energy per unit mass. Pulliam and Steger use  $\bar{z}$  as the coordinate normal to the surface, and  $\bar{y}$  as the spanwise coordinate. In order to minimize code changes, we use this coordinate system in the numerical computations and then, at the end, change  $\bar{z}$  to  $y$ ,  $\bar{w}$  to  $v$ ,  $\bar{y}$  to  $x$ , and  $\bar{v}$  to  $w$  in order to present results in the more familiar boundary layer coordinate designations. We employ simple cartesian coordinates in the streamwise  $x$ - and spanwise  $y$ -directions, and a stretched mesh in the normal  $z$  direction in order to concentrate points both near the wall and the outer edge. The metrics for the transformation are  $\xi_x = 1, \eta_y = 1/\Delta\bar{y}_+, \zeta_z = 1/\Delta\bar{z}_+$  where  $\Delta\bar{y}_+$  and  $\Delta\bar{z}_+$  are the mesh spacings in wall units in the spanwise and normal directions respectively.

The same basic physical approximation is made as in Chapman and Kuhn (1981), namely, that coherent sublayer eddy structures are highly elongate stream-

wise. In our case we assume—in accordance with experimental observations (e.g. Iritani et. al (1981)) — that the temperature eddies are also highly elongate streamwise. In the notation of Pulliam and Steger, the corresponding divergence form of the Navier–Stokes equations is

$$\partial_t \hat{q} = \partial_\eta (\hat{F}_v - \hat{F}) + \partial_\zeta (\hat{G}_v - \hat{G}) + \partial_\xi \hat{F}_p \quad (1)$$

where the vectors  $\hat{F}$ ,  $\hat{F}_v$ ,  $\hat{G}$ ,  $\hat{G}_v$  and  $\hat{q}$  are identical to the conventional ones used by Pulliam and Steger for the case of orthogonal coordinates corresponding to the metrics of equation (1). However, the vector

$$\hat{F}_p = J^{-1} \begin{bmatrix} 0 \\ p_e \\ 0 \\ 0 \\ \frac{\gamma}{\gamma-1} p_e \xi_x u_e \end{bmatrix} \quad (2)$$

differs from theirs due to our assumption of highly elongate eddies in the streamwise direction. Thus, streamwise derivatives other than the mean streamwise pressure gradient  $dp_e/dx$  are neglected relative to derivatives in the spanwise and normal directions.

This basic approximation, which involves computation of 3 velocity components in 2 space directions, has been variously termed “2.5D flow”, or “slender turbulence theory”, or “slender eddy theory.”

Since Pulliam and Steger used the thin-layer form of the Navier–Stokes equations, we write, in order to retain a tridiagonal structure,

$$\begin{aligned} \frac{\partial(\hat{F}_v - \hat{F})}{\partial q} &= \frac{\partial \hat{F}}{\partial q} = A_o + A_x \\ \frac{\partial(\hat{G}_v - \hat{G})}{\partial q} &= \frac{\partial \hat{G}}{\partial q} = B_o + B_x \end{aligned} \quad (3)$$

where the matrices  $A_o$  and  $B_o$  contain no cross derivative terms, while  $A_x$  and  $B_x$  contain all such terms. The detailed structure of these matrices is given in Appendix I. Our basic factored algorithm becomes

$$\begin{aligned} (I - \frac{2}{3}h\delta_\eta A_o^n)(I - \frac{2}{3}h\delta_\zeta B_o^n)\Delta\hat{q}^{n+1} = & \frac{2}{3}h[\delta_\eta F^n + \partial_\zeta G^n] + \frac{2}{3}h\partial_\eta A_x^n \Delta q^n \\ & + \frac{2}{3}h\delta_\zeta B_x^n \Delta q^n + \frac{2}{3}h\delta_\xi \hat{F}_p + \frac{1}{3}\Delta\hat{q}^n \end{aligned} \quad (4)$$

this differs from the Pulliam-Steger algorithm by the addition of the last four terms on the right hand side. Of these, the last one corresponds to a three-point backward Euler difference scheme for time derivatives (added for accuracy and stability reasons explained later); the next to last term corresponds to body pressure gradients imposed by the large scale eddies, while the third and fourth from last represent the additional terms required for the full Navier-Stokes equations in place of the thin-layer equations used by Pulliam and Steger.

### BOUNDARY CONDITIONS

The primary element in formulating our computational model involves the construction of realistic time- and space-dependent boundary conditions for the fluctuating temperature  $\theta$  and the fluctuating velocity components  $u$ ,  $v$ ,  $w$  at the outer edge of the viscous sublayer. Various experimental observations are used as a guide to this construction. Computations using the time-dependent Navier-Stokes equations are then made over a length of time long enough for the various statistical quantities, e.g., mean values, correlation coefficients, rms fluctuating intensities, etc., to reach a periodic state within the viscous sublayer.

Our general approach is an extension of that employed by Chapman and Kuhn (1981) for incompressible flow without heat transfer. They considered two coherent components of turbulent motion at the outer edge of the viscous sublayer (lower

edge of the logarithmic region). One component represents the small scale eddies (SSE) responsible for the principal production of turbulence and Reynolds stress. A second component represents the organized large scale eddies (LSE) which interact with the small scale eddies. They used a simple initial construction for purposes of illustrating the potential and main characteristics of this type of turbulence modeling. With all quantities expressed in conventional dimensionless wall variables, their velocity boundary conditions for the outer edge of the viscous sublayer were

<u>Component 1-SSE</u>	<u>Component 2-LSE</u>	
$u_{e+} = 2\alpha_1 \sin N_1 T \sin \zeta$	$+ \sqrt{2(\alpha^2 - \alpha_1^2)} \sin(N_{u2}T + \phi_{u2})$	
$v_{e+} = -2\beta \sin N_1 T \sin \zeta$		(5)
$w_{e+} = 2\beta \cos N_1 T \cos \zeta$	$+ \sqrt{\gamma^2 - \beta^2} \sin\left(\frac{N_{w2}}{2}T + \phi_{w2}\right)$	

where  $\alpha$ ,  $\beta$ ,  $\gamma$  are the rms intensities of fluctuation of  $u_{e+}$ ,  $v_{e+}$ ,  $w_{e+}$ , respectively,  $N_1$  is the mean frequency of SSE burst events (ejection/sweep events),  $N_{u2}$  is the mean frequency of LSE,  $\zeta = 2\pi z/\lambda$  is a dimensionless spanwise distance variable,  $T$  is the dimensionless time,  $\lambda$  is the mean spacing between high-speed or low-speed streaks,  $\alpha_1/\alpha$  is the  $uv$  correlation coefficient (0.45), and  $\phi_{u2}$  and  $\phi_{w2}$  are phase angles. The flow model is periodic both in time and span. Hence the boundary conditions for the spanwise side walls of the computational domain were

$$\begin{aligned}
 u_{e+}(y, 0, t) &= u_{e+}(y, \lambda, t) \\
 v_{e+}(y, 0, t) &= v_{e+}(y, \lambda, t) \\
 w_{e+}(y, 0, t) &= w_{e+}(y, \lambda, t)
 \end{aligned}
 \tag{6}$$

and at the surface

$$u_{e+}(0, z, t) = v_{e+}(0, z, t) = w_{e+}(0, z, t) = 0$$

This construction of velocity boundary conditions was guided by experimental observations of organized sublayer structure. For example, the  $\sin \zeta$  factor for  $u_{e+}$  corresponds to the observation of high- and low-speed streaks spaced spanwise a mean distance of  $\lambda$  apart, while the factors  $\sin \zeta$ ,  $\sin \zeta$ ,  $\cos \zeta$  in the  $u_{e+}$ ,  $v_{e+}$ ,  $w_{e+}$  equations, respectively, correspond to a simple modeling of the observations of contra-rotating vortical motion near a wall. The absence of a phase angle in time between  $u_{e+}$  and  $v_{e+}$  corresponds to the observation that the  $u-v$  correlation in the log region is maximum with zero time delay between their respective signals. The  $180^\circ$  phase difference between  $u_{e+}$  and  $v_{e+}$  corresponds to observations from conditional samples in the sublayer that  $u$  and  $v$  are  $180^\circ$  out of phase during the Reynolds-stress intensive ejection-sweep event. The  $90^\circ$  phase difference in time between  $v_e$  and  $w_e$  corresponds to the observation that the derivative  $(\partial \overline{v^2} / \partial y_+)_e$  at the outer edge of the viscous sublayer is zero. A comparison of a number of turbulence characteristics computed from this simple model with those measured in experiments showed surprisingly good agreement. This model was developed for flows with a mean streamwise pressure gradient, although numerical computations were made by Chapman and Kuhn only for the relatively small pressure gradients that exist in incompressible pipe and channel flow.

The above two-component velocity boundary conditions at the outer edge of the viscous sublayer are fully compatible with the concept of "active" and "inactive" components of turbulent motion in the log region as characterized by Townsend (1961) and Bradshaw (1967). Component 1 is active, involving small scale eddies, producing the Reynolds stress, being rotational, and being dependent on wall variables. Component 2 is inactive, involving large-scale eddies, producing

energy but no Reynolds stress, being irrotational, and being dependent on outer variables. There is much experimental information that turbulent flow in the log region, and hence at the outer edge of the viscous sublayer, comprises these two distinct types of motion.

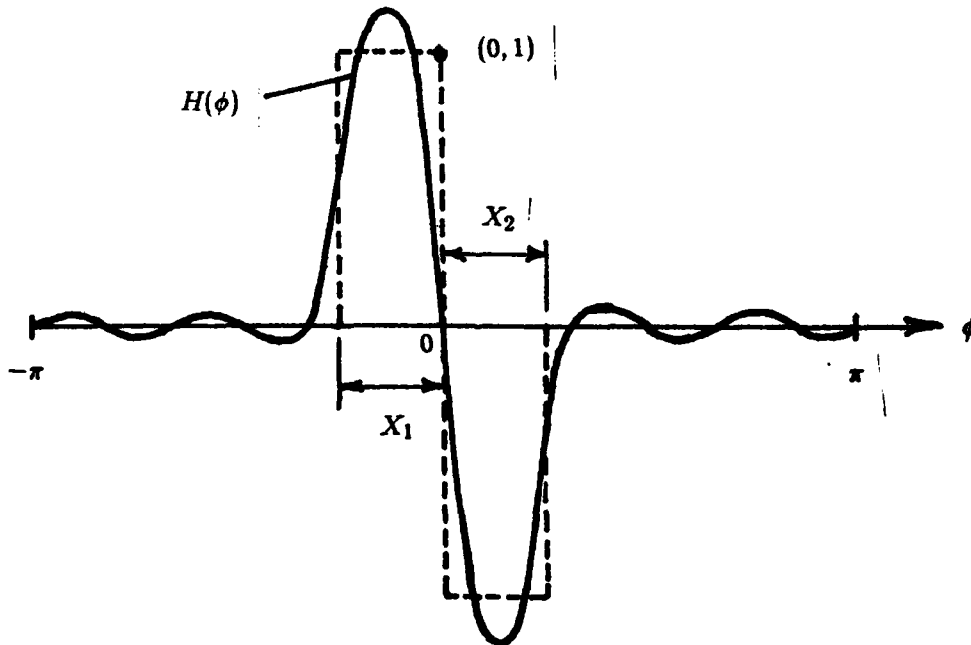
The computational model of Chapman and Kuhn is not regarded as sufficiently realistic for purposes such as outlined in the section above on motivations. Their results do illustrate, however, that the general approach employed has the potential of eventually leading to a sufficiently realistic model. Towards this end, it is believed that at least three additional aspects of turbulence physics will have to be introduced into the model. First, production of Reynolds stress should be intermittent in time, rather than sinusoidal-like as in boundary conditions (5). Second, conditional samples for  $v(t)$  in ejection/sweep events indicate that the  $v^2$  turbulent energy contained in these SSE events should be only a fraction of the total  $v^2$  energy, rather than the entire amount as in equation (5). Third, visualizations of viscous sublayer flow exhibit a mixture of order and disorder, rather than coherent order only. To date, in work supported by another contract, progress has been made on modifying the outer edge velocity boundary conditions to account for the first two of these three physical aspects. We will incorporate this progress into our velocity boundary conditions. In addition, for the heat transfer case we must also construct an appropriate boundary condition for the fluctuating temperature  $\theta_e$  at the outer edge of the viscous sublayer.

One important guide to the construction of boundary conditions is provided by measurements of spectral density  $f$ . Fortunately, spectra for  $\theta$ ,  $u$ ,  $v$ , and  $w$ , have been obtained by Fulachier (1972) at  $y$ -positions near the outer edge of the viscous sublayer. Data for  $y_{e+} \approx 40$  (interpolated between his measurements at  $y_+ = 31$  and 77) are shown in figure 2. Since

$$\int_0^{\infty} f dk = \int_0^{\infty} k f d(\ln k) = 1$$

the areas under curves of  $u^2 k f_u$ ,  $v^2 k f_v$ , and  $w^2 k f_w$  versus  $\log k$  are proportional to the relative amounts of kinetic energy in these velocity components. Along the wave number scale  $k$ , pips are shown corresponding to LSE eddy scales of  $\pi/\delta$  (where  $\delta$  is the boundary layer thickness) and to SSE eddy scales of  $\pi/\lambda$ . It is seen that, whereas both  $u$  and  $\theta$  exhibit eddy scales ranging from large [ $O(\delta)$ ] to small [ $O(\lambda)$ ],  $v$  exhibit scales ranging only from medium [ $O(\text{several } \lambda)$ ] to small. Our boundary conditions will be constructed to be as consistent as possible with experimental data of this type.

A relatively simple method (developed under a separate contract) is used to simulate the intermittent character of Reynolds-stress production. Since  $\bar{u}\bar{v}$  is produced only by the active component of small scale eddies (SSE), only the time functions  $\sin N_1 T$  and  $\cos N_1 T$  in equation (1) need be modified. For this purpose we use a simple Fourier series approximation  $H(\phi)$  to a rectangular pulse function, where  $\phi \equiv N_1 T$ .



For  $M$  terms in the approximating Fourier series, we have

$$\begin{aligned}
 H(\phi) &= \sum_1^M (a_n \cos n\phi + b_n \sin n\phi) \\
 \overline{H^2} &= \frac{1}{2} \sum_1^M (a_n^2 + b_n^2) \\
 a_n &= \frac{1}{\pi n} \left[ \sin nX_1 - \frac{X_1}{X_2} \sin nX_2 \right] \\
 b_n &= \frac{1}{\pi n} \left[ \frac{X_1}{X_2} (\cos nX_2 - 1) + (\cos nX_1 - 1) \right]
 \end{aligned} \tag{7}$$

values of  $M$  in the range of 3 to 5 are anticipated. Since the skewness of the rectangular pulse function is

$$S_e = \sqrt{\frac{2\pi}{X_1 X_2} \frac{(X_2 - X_1)}{\sqrt{X_2 + X_1}}}$$

we can build skewness into  $H(\phi)$  simply by having  $X_2$  different from  $X_1$ . Initial computations, however, are planned for zero skewness at the outer edge, and with  $X_1 = X_2 = 0.25\pi$ , since hot-wire measurements have indicated that the principal  $\overline{uv}$  is produced in about 25% of the time, with relative  $\overline{uv}$  quiescence the remaining 75% of time.

In conventional wall variables, the outer edge boundary conditions constructed to date include terms representing small scale eddies (SSE) of length scale  $\lambda$ , large scale eddies (LSE) of length scale  $\geq 10\lambda$ , and medium scale eddies (MSE) of intermediate length scale  $3\lambda$ . Computations are made within a domain covering 3 spanwise cells each  $\lambda$  in width. The LSE are treated as being of sufficiently large scale that their time-dependent velocity component does not vary across the spanwise extent of the computational domain. The equation of continuity precludes having a LSE component in the boundary condition for  $v_e$ .

SSE	LSE	MSE
Scale $\lambda$	Scale $> 10\lambda$	Scale $3\lambda$

$$\begin{aligned}
u_e &= \sqrt{2}\alpha_1 F_u(\phi) \sin \zeta + \sqrt{2(\alpha^2 - \alpha_1^2)} \sin(N_{u2}T + \phi_{u2}) \\
v_e &= \sqrt{2}\beta_1 F_v(\phi) \sin \zeta + 2\beta_2 \sin(3N_{u2}T) \sin \frac{\zeta}{3} \\
w_e &= \sqrt{2}\beta_1 F_w(\phi) \cos \zeta + \sqrt{2(\gamma^2 - \beta_1^2)} \sin\left(\frac{N_{u2}T}{2} + \phi_{w2}\right)
\end{aligned}
\tag{8}$$

$$\theta_e = \sqrt{2}a_1 F_\theta(\phi) \sin \zeta + \sqrt{2(a^2 - a_1^2)} \sin(N_{u2}T + \phi_{\theta 2})$$

where, in addition to the quantities already defined,  $a \equiv \sqrt{(\theta^2)_e}$ ,  $\phi_{\theta 2}$  is a phase angle in the large-eddy component of temperature, and

$$\begin{aligned}
F_\theta(\phi) &= -F_u(\phi) = F_v(\phi) = \frac{H(\phi)}{\sqrt{H^2(\phi)}} \\
F_w(\phi) &= -\frac{H(\phi + \phi_{w1})}{\sqrt{H^2(\phi + \phi_{w1})}}
\end{aligned}$$

are the intermittent time functions normalized such that  $\overline{F^2} = 1$ . The boundary conditions for the spanwise side walls of the computational domain are

$$\begin{aligned}
u_{e+}(y, 0, t) &= u_{e+}(y, 3\lambda, t) \\
v_{e+}(y, 0, t) &= v_{e+}(y, 3\lambda, t) \\
w_{e+}(y, 0, t) &= w_{e+}(y, 3\lambda, t)
\end{aligned}$$

Thus the computation allows for flow interaction between the center cell and the two outside cells unconstrained by specific boundary conditions.

As in the model of Chapman and Kuhn:  $\alpha$ ,  $\beta$ ,  $\gamma$ ,  $\alpha$  are determined from experimental data on the intensities of turbulence fluctuations in wall units at the outer edge of the viscous sublayer ( $\alpha \approx 2, \beta \approx 1, \gamma \approx 1.3, \alpha \approx 1.3$ );  $\phi_{w2}$ ,  $\phi_{\theta 2}$ ,  $\phi_{u2}$ , are determined by computer trial to conform to the mean-velocity law of the wall, mean-temperature law of the wall, and  $u$ -velocity skewness, respectively;  $\phi_{w1}$  is determined analytically by the requirement that  $(\partial \overline{v^2} / \partial y)_e$  is zero;  $\alpha_1$  is determined by the correlation coefficient  $0.45 = -(R_{uv})_e = \alpha_1 \beta_1 / \alpha \beta$ ;  $a_1$  is determined by the correlation coefficient  $0.8 \approx -(R_{u\theta})_e = \frac{\alpha_1 a_1}{\alpha a} + \frac{1}{\alpha a} \sqrt{(\alpha^2 - \alpha_1^2)(a^2 - a_1^2)} \cos(\phi_{\theta 2} - \phi_{u2})$ ; and  $\beta_1 / \beta$  is determined from conditional samples of the ejection/sweep event. This latter determination is made by assuming that the peak to peak amplitude ratio  $\langle v \rangle_{ppa} / \langle u \rangle_{ppa}$ , from the conditional samples is equal to the ratio  $\beta_1 / \alpha_1$ , and then using the above equation for  $(R_{uv})_e$  to compute both  $\beta_1 / \beta$  and  $\alpha_1 / \alpha$ . An independent determination of  $\alpha_1 / \alpha$  has been made from direct measurements of the fraction of total  $u^2$  energy that exists during bursts, and hence also of  $\beta_1 / \beta$  from the equation for  $(R_{uv})_e$ . Still a different determination has been made from  $\langle w \rangle_{ppa} / \langle u \rangle_{ppa} = \beta_1 / \alpha_1$  coupled with the equation for  $(R_{uv})_e$ . Results of these determinations (made on a separate contract) are:

Data Source	Method	$\beta_1 / \beta$
Chen & Blackwelder (1978)	$\langle v \rangle / \langle u \rangle$ plus $R_{uv} = -.45$	.53
Nakagawa & Nezu (1981)	$\langle v \rangle / \langle u \rangle$ plus $R_{uv} = -.45$	.72
Blackwelder & Kaplan (1979)	$\langle v \rangle / \langle u \rangle$ plus $R_{uv} = -.45$	.49
Kim (1982)	$\langle u \rangle / \langle u \rangle$ from LES computations, plus $R_{uv} = -.45$	.60
Kim, Kline & Reynolds (1971)	Fraction of total $u^2$ energy during bursts (.68), plus $R_{uv} = -.45$	.59
Blackwelder & Kaplan (1979)	$\langle w \rangle / \langle u \rangle$ plus $R_{uv} = -.45$	.64

On average, the value of  $\beta_1 / \beta$  appears to be near 0.6.

It is to be noted that the structure of boundary conditions (8) comprises in equal proportions both ejection/sweep events (where a sweep follows an ejection), and

sweep/ejection events (where an ejection follows a sweep). The recent experiments of Johansson and Alfredsson (1982) clearly reveal that both types of event occur. Their experimental VITA data for the smallest threshold values and the longest integration times employed, indicate these two event types to be about equally numerous. Both types have also been observed visually by Offen and Kline (1974) who use the term "cleansing sweep" in an ejection/sweep event to distinguish from sweeps in a sweep/ejection event.

## STATUS OF RESEARCH

As outlined above, research on formation of the differential equations and the initial trial boundary conditions is completed. We also have (1) essentially completed a survey of various existing theories for turbulent Prandtl number, and have (2) made most of the programming modifications necessary to utilize the Pulliam-Steger code in our computational model. Some details of progress in these latter two areas are presented in the sections which follow.

### Survey of various theories for $Pr_t$

Without a reliable guide from experiment as to how  $Pr_t$  should be modeled near a wall, the various theoretical models advanced to date have differed greatly. This is illustrated in figures 3, 4, and 5 showing our compilation of various theories for fluids of molecular Prandtl number 0.72 (air), 6 (water), and 1000 (oil), respectively. Our survey of existing theories is near completion, although not yet fully complete. The various theories explored clearly demonstrate that a very wide range of uncertainty exists for  $Pr_t$  in the viscous sublayer. Present theories do not attempt to define how  $Pr_t$  may vary with pressure gradient.

### Programming of Navier-Stokes Code

Our plan is to develop a single Navier-Stokes code which can be used either for low-speed subsonic flows ( $M \ll 1$ ) with heat transfer, or for high Mach number flows. Since the Pulliam-Steger code was written for the thin-layer approximation to the Navier-Stokes equations, a number of programming modifications are required to adapt this code to the computation of viscous sublayer dynamics. These are:

1. Change variables from free stream reference to nondimensional wall variables.
2. Add subroutine for the boundary conditions on velocity and temperature fluctuations at the outer edge of the viscous sublayer.
3. Change the time-derivative algorithm to a stable, second-order accurate algorithm.
4. Add the spanwise viscous stress terms, plus the associated cross derivatives terms.
5. Add a global streamwise pressure gradient term, associated with the large scale eddies, to the right hand side of the basic algorithm.
6. Add a block periodic solver for the spanwise direction.
7. Add appropriate nonperiodic terms in the spanwise boundary conditions for  $\rho$ ,  $p$ ,  $T$ .

An outline of the progress status of each of these seven items is given in the sections which follow.

1. Completed
2. Subroutine coding of the boundary conditions for the initial test case has been completed. This case comprises the same velocity boundary conditions as

used by Chapman and Kuhn (1981), plus a temperature boundary condition representing small-scale and large-scale eddy components. The subroutine will be used to check results against the previous results of Chapman and Kuhn for low-speed subsonic flow without heat transfer. Once a check is obtained, a modified boundary-conditions subroutine will be written to represent boundary conditions (8) which simulate intermittent Reynolds stress production, rather than the sinusoidal-like production contained in the Chapman-Kuhn boundary conditions (5).

3. **Completed.** In order to test the algorithm accuracy for the time derivative terms, an exact analytical solution was derived for incompressible oscillating shear flow with heat transfer. This solution is an extension of the Chapman-Kuhn solution for flow without heat transfer. Mathematical details of the analytical solution are presented in Appendix II. It was found that neither of the two option algorithms in the Pulliam-Steger code (i.e., Euler implicit first order, or trapezoidal second order) were sufficiently accurate and stable. With helpful guidance from Dr. Pulliam, a three-point backward Euler algorithm was coded and found to be satisfactory. The very close agreement obtained with this second-order accurate algorithm, between numerical computations and the exact analytical solution, is illustrated in figures 6 and 7 for the adiabatic-wall case and the heat-transfer case, respectively. Since oscillating shear flow with heat transfer involves viscous and heat-conduction terms as well as time-derivative terms, this test flow provides a check on the accuracy of the numerics for all three types of terms. It does not provide, however, a check on the accuracy of the convection terms which are zero in oscillating shear flow.
4. **Completed**
5. **Completed**

6. Completed

7. Not yet undertaken. This coding modification apparently is not needed for low speed subsonic flows. The necessary code changes are not planned to be undertaken until we begin to model high Mach number flows. With fluctuations in spanwise body pressure gradient, all three velocity components remain periodic spanwise, but the state variables  $p$ ,  $\rho$ ,  $\theta$  do not. The linear body pressure gradients create step discontinuities at the spanwise boundary points. This can induce numerical oscillations near the boundaries with the central differencing scheme used. At low subsonic Mach numbers these discontinuities are very small, so that the block periodic solver can be used with little problem. At high Mach numbers, however, the relative pressure fluctuations  $\Delta p/p$  increase, and the magnitude of the step discontinuities can increase sufficiently to cause numerical problems if periodic boundary conditions are imposed on the state variables. Our plan to handle this for high speed flows is to decompose  $p$ ,  $\rho$  and  $T$  into a spanwise periodic component determined by small scale eddies, plus a nonperiodic component determined by large scale eddies. The latter would be included as a right-hand-side term, and the overall set of equations cast into a form for which periodic boundary conditions are applicable.

## PROGRESS SUMMARY

*During the first contract year (CY 1982) we have made progress as follows:*

- Survey of theories for  $Pr_t$  essentially complete.
- Exact analytical solution derived for incompressible oscillating shear flow with heat transfer.
- Using analytical solution, satisfactory test conducted on accuracy of numerical algorithms for time-dependent, heat-conduction, and viscous terms.
- Most necessary programming modifications to the Pulliam-Steger Navier-Stokes code completed (but not yet debugged).
- A boundary condition for fluctuating temperature has been formulated for initial trial computations.

*Some of the subsequent steps to be conducted in CY 1983 are:*

- Complete necessary programming modifications to Pulliam-Steger code (e.g. various statistical space-time averages for fluctuation intensities, correlations, skewness, flatness, dissipation, Reynolds stresses, etc.
- Debug code and run check case for incompressible flow without heat transfer using same boundary conditions as employed by Chapman and Kuhn.
- Make computer runs to develop temperature boundary conditions that are as realistic as possible, testing computations against experimental data.
- Make computer runs for fluids of various molecular Prandtl number and stream-wise pressure gradient.

## REFERENCES

- Blackwelder, R. F. and Kaplan, R.E. (1976): On the Wall Structure of the Turbulent Boundary Layer. *Jour., Fluid Mech.*, **76**, Pt 1, pp 89-112.
- Bradshaw, P. (1967): "Inactive" Motions and Pressure Fluctuations in Turbulent Boundary Layers. *Jour. Fluid Mech.*, **30**, pt 2, pp 241-258.
- Cantwell, B.J. (1981): Organized Motion in Turbulent Flow. *Ann. Rev. Fluid Mech.*, **13**, pp 457-515.
- Chapman, D.R. (1980): Trends and Pacing Items in Computational Aerodynamics. *Lecture Notes in Physics*, Springer-Verlag, **141**, pp 1-11.
- Chapman, D.R. and Kuhn, G.D. (1981): Two-Component Navier-Stokes Computational Model of Viscous Sublayer Turbulence. AIAA paper 81-1024, Proc. 5th CFD Conference, Palo Alto, Ca.
- Chen, C.H. and Blackwelder, R. (1978): Large-Scale Motion in a Turbulent Boundary layer: A Study using Temperature Contamination. *Jour. Fluid Mech.*, **89**, Pt 1, pp 1-31.
- Clark, R.A., Ferziger, J.H. and Reynolds, W.C. (1979): Evaluation of Subgrid-Scale Models Using Accurately Simulated Turbulent Flow. *Jour. Fluid Mech.*, **91**, Pt 1, pp 1-16.
- Fulachier, L. (1972): Contribution a L'Etude des Analogies des Champs Dynamique et Thermique dans une Couche Limite Turbulent. Effet de L'Aspiration. *Thesis*, University of Provence, France.
- Iritani, Y., Kasagi, N., and Hirata, H. (1981): Transport Mechanism in a Turbulent Boundary Layer-Visualized Behavior or Wall Temperature by Liquid Crystal. Submitted to *Trans. JSME (B)*.
- Johansson, A.V. and Alfredsson, P.H. (1982): On the Structure of Turbulent Channel Flow. *Jour. Fluid Mech.*, **122**, pp 295-314.

Kim, J. (1982): On the structure of Wall Bounded Turbulent Flows. Paper presented at Amer. Phys. Soc. Division of Fluid Dynamics Meeting, Rutgers Univ., Nov. 21-23, 1982.

Kim, H.T., Kline, S.J., and Reynolds, W.C. (1971): The Production of Turbulence Near a Smooth Wall in a Turbulent Boundary Layer. Jour. Fluid Mech., 50, pt 1, pp 133-160.

McMillan, O.J. and Ferziger, J.H. (1979): Direct Testing of Subgrid-Scale Models. AIAA Paper 79-0072.

Nakagawa, H. and Nezu, I. (1981): Structure of Space-time Correlations of Bursting Phenomena in an Open Channel Flow, Jour. Fluid Mech., 104, pp 1-43.

Offen, G.R. and Kline, S.J. (1974): Combined Dye-Streak and Hydrogen-Bubble Visual Observations of a Turbulent Boundary Layer. Jour. Fluid Mech., 62, pt 2, pp 223-239.

Patel, V.C. Rodi, W. and Scheuerer, G. (1981): Evaluation of Turbulence Models for Near-Wall and Low-Reynolds Number Flows. Proc. Third Symposium on Turbulent Shear Flows, Sept. 9-11, 1981, pp 1.1-1.8.

Pulliam, T.H. and Steger, J.L. (1980) Implicit Finite Difference Simulations of Three-Dimensional Compressible Flow. AIAA jour., 18, pp 149-158.

Rogallo, R. (1977): An ILLIAC Program for the Numerical Simulation of Homogeneous Incompressible Turbulence. NASA TM NO. 73, 203.

Shirani, E., Ferziger, J.H. and Reynolds, W.C. (1981): Mixing of a Passive Scalar in Isotropic and Sheared Turbulence. Report No. TF-15, Thermosciences Division, Dept. Mechanical Engineering, Stanford University.

Simpson, R.L., Whitten, D.G. and Moffatt, R.J.: An Experimental Study of the Turbulent Prandtl Number of Air with Injection and Suction. Int. J. heat and Mass Transfer, 13, pp 125-143.

Townsend, A.A. (1961): Equilibrium Layers and Wall Turbulence. *Jour. Fluid Mech.*, 11, pp 97-120.

## APPENDIX I

### DECOMPOSITION MATRICES

The derivatives  $\partial\hat{F}/\partial q$  and  $\partial\hat{G}/\partial q$  are each decomposed into two matrices, one (subscript zero) that does not contain cross derivative terms, and another (subscript  $x$ ) that contains all such terms.

$$\frac{\partial\hat{F}}{\partial q} = A_o + A_x$$

$$\frac{\partial\hat{G}}{\partial q} = B_o + B_x$$

where the matrix  $A_o$  is

$$A_o = - \begin{vmatrix} 0 & 0 & \eta_y & 0 & 0 \\ -u\eta_y v & \eta_y v & \eta_y u & 0 & 0 \\ \eta_y(\phi^2 - v^2) & -\eta_y(\gamma - 1)u & -\eta_y v(\gamma - 1) & -\eta_y(\gamma - 1)w & \eta_y(\gamma - 1) \\ -w\eta_y v & 0 & \eta_y w & \eta_y v & 0 \\ \eta_y v \left[ 2\phi^2 - \gamma \frac{\epsilon}{\rho} \right] & -(\gamma - 1)u\eta_y v & \left. \begin{matrix} -(\gamma - 1)\eta_y v^2 + \\ \eta_y \left[ \gamma \frac{\epsilon}{\rho} - \phi^2 \right] \end{matrix} \right\} & -(\gamma - 1)w\eta_y v & \gamma\eta_y v \end{vmatrix}$$

$$+ \frac{J-1}{Re} \begin{vmatrix} 0 & 0 & 0 & 0 & 0 \\ -\sigma_1 \delta_\eta(u/\rho) & \sigma_1 \delta_\eta\left(\frac{1}{\rho}\right) & 0 & 0 & 0 \\ -\sigma_2 \delta_\eta(v/\rho) & 0 & \sigma_2 \delta_\eta\left(\frac{1}{\rho}\right) & 0 & 0 \\ -\sigma_1 \delta_\eta(w/\rho) & 0 & 0 & \sigma_1 \delta_\eta\left(\frac{1}{\rho}\right) & 0 \\ \left. \begin{matrix} (\sigma_5 - \sigma_1) \delta_\eta \left[ \frac{u^2 + w^2}{\rho} \right] \\ + (\sigma_5 - \sigma_2) \delta_\eta \left( \frac{v^2}{\rho} \right) - \sigma_5 \delta_\eta \left( \frac{\epsilon}{\rho^2} \right) \end{matrix} \right\} & (\sigma_1 - \sigma_5) \delta_\eta\left(\frac{u}{\rho}\right) & (\sigma_2 - \sigma_5) \delta_\eta\left(\frac{v}{\rho}\right) & (\sigma_1 - \sigma_5) \delta_\eta\left(\frac{w}{\rho}\right) & \sigma_5 \delta_\eta\left(\frac{1}{\rho}\right) \end{vmatrix}^J$$

$$\phi^2 = \frac{1}{2}(\gamma - 1)(u^2 + v^2 + w^2)$$

$$s_1 = \mu\eta_y^2 \quad s_2 = \frac{4}{3}s_1 \quad s_5 = \frac{\gamma}{P_r}s_1$$

$$Re = \frac{a_w \delta}{\nu_w} = \frac{\sqrt{\gamma R \theta_w} \delta}{\nu_w}$$

$$J = \text{Jacobian} = \frac{1}{\Delta y + \Delta z}$$

and the matrix  $A_x$  is

$$A_x = \begin{vmatrix} 0 & 0 & 0 & 0 & 0 \\ 0 & 0 & 0 & 0 & 0 \\ -s_4 \delta_\zeta \left(\frac{w}{\zeta}\right) & 0 & 0 & s_4 \delta_\zeta \left(\frac{1}{\rho}\right) & 0 \\ -s_3 \delta_\zeta \left(\frac{v}{\rho}\right) & 0 & s_3 \delta_\zeta \left(\frac{1}{\rho}\right) & 0 & 0 \\ \left\{ \begin{array}{l} -s_3 \left[ \frac{w}{\rho} \delta_\zeta v + w \delta_\zeta \left(\frac{v}{\rho}\right) \right] \\ -s_4 \left[ \frac{v}{\delta} \delta_\zeta w + v \delta_\zeta \left(\frac{w}{\rho}\right) \right] \end{array} \right\} & 0 & s_4 \frac{1}{\rho} \delta_\zeta w + s_3 w \delta_\zeta \left(\frac{1}{\rho}\right) & s_4 v \delta_\zeta \left(\frac{1}{\rho}\right) + s_3 \frac{1}{\rho} \delta_\zeta v & 0 \end{vmatrix}$$

$$s_3 = \mu\eta_y s_z$$

$$s_4 = -\frac{2}{3}s_3$$

The matrix  $B_o$  is

$$B_o = \begin{vmatrix} s_z w & 0 & 0 & s_z & 0 \\ -u s_z w & s_z w & 0 & s_z u & 0 \\ -v s_z w & 0 & 0 & s_z v & 0 \\ s_z \phi^2 - w^2 s_z & -s_z(\gamma - 1)u & -s_z(\gamma - 1)v & -s_z(\gamma - 2)w & s_z(\gamma - 1) \\ s_z w \left[ 2\phi^2 - \gamma \frac{\epsilon}{\rho} \right] & -(\gamma - 1)u s_z w & -(\gamma - 1)v s_z w & s_z \left[ \gamma \frac{\epsilon}{\rho} - \phi^2 - (\gamma - 1)w^2 \right] & \gamma s_z w \end{vmatrix} +$$

$$+\frac{J-1}{Re} \left\{ \begin{array}{ccccc} 0 & 0 & 0 & 0 & 0 \\ -T_1 \delta_\zeta \left( \frac{u}{\rho} \right) & T_1 \delta_\zeta \left( \frac{1}{\rho} \right) & 0 & 0 & 0 \\ -T_1 \delta_\zeta \left( \frac{v}{\rho} \right) & 0 & T_1 \delta_\zeta \left( \frac{1}{\rho} \right) & 0 & 0 \\ -T_2 \delta_\zeta \left( \frac{w}{\rho} \right) & 0 & 0 & T_2 \delta_\zeta \left( \frac{1}{\rho} \right) & 0 \\ (T_5 - T_1) \delta_\zeta \left( \frac{u^2 + v^2}{\rho} \right) & (T_1 - T_5) \delta_\zeta \left( \frac{u}{\rho} \right) & (T_1 - T_5) \delta_\zeta \left( \frac{v}{\rho} \right) & (T_2 - T_5) \delta_\zeta \left( \frac{w}{\rho} \right) & T_5 \delta_\zeta \left( \frac{1}{\rho} \right) \\ + (T_5 - T_1) \delta_\zeta \left( \frac{w^2}{\rho} \right) - T_5 \delta_\zeta \left( \frac{\epsilon}{\rho^2} \right) & & & & \end{array} \right\} \quad J$$

$$T_1 = \mu \zeta^2 \quad T_2 = \frac{4}{3} T_1 \quad T_5 = \frac{7}{Pr} T_1$$

and the matrix  $B_x$  is

$$B_x = \left\{ \begin{array}{ccccc} 0 & 0 & 0 & 0 & 0 \\ 0 & 0 & 0 & 0 & 0 \\ -s_3 \delta_\eta \left( \frac{w}{\rho} \right) & 0 & 0 & s_3 \delta_\eta \left( \frac{1}{\rho} \right) & 0 \\ -s_4 \delta_\eta \left( \frac{v}{\rho} \right) & 0 & s_4 \delta_\eta \left( \frac{1}{\rho} \right) & 0 & 0 \\ \left[ -s_3 \left[ \frac{v}{\rho} \delta_\eta w + v \delta_\eta \left( \frac{w}{\rho} \right) \right] \right] & 0 & s_4 w \delta_\eta \left( \frac{1}{\rho} \right) + s_3 \frac{1}{\rho} \delta_\eta w & s_3 v \delta_\eta \left( \frac{1}{\rho} \right) + s_4 \frac{1}{\rho} \delta_\eta v & 0 \\ \left[ -s_4 \left[ \frac{w}{\rho} \delta_\eta v + w \delta_\eta \left( \frac{v}{\rho} \right) \right] \right] & & & & \end{array} \right\}$$

## APPENDIX II

An exact analytical solution has been derived for oscillating shear flow with heat transfer in an incompressible fluid with constant properties. Since the momentum equations are independent of the thermal energy equation in incompressible flow, the velocity field is the same as for the case without heat transfer derived by Chapman and Kuhn (1981). With  $y$  as the coordinate normal to the infinite flat surface, and  $u$  and  $v$  as the velocity components in the streamwise and spanwise directions, respectively, we have

$$u = A \left[ \sin nt - e^{-k_n y} \sin(nt - k_n y) \right] + cy$$

$$v = B \left[ \sin(mt + \phi) - e^{-k_m y} \sin(mt - k_m y) \right]$$

where

$$k_n = \sqrt{\frac{n}{2\nu}} \quad k_m = \sqrt{\frac{m}{2\nu}}$$

The oscillating frequencies are  $n$  in the streamwise direction and  $m$  in the spanwise direction, and the mean velocity profile is  $\bar{u} = cy$ . For this velocity field, the solution to the thermal energy equation

$$\rho c_p \frac{\partial \theta}{\partial t} = k \frac{\partial^2 \theta}{\partial y^2} + \mu \left[ \left( \frac{\partial u}{\partial y} \right)^2 + \left( \frac{\partial v}{\partial y} \right)^2 \right]$$

is

$$\begin{aligned} T(z, t) = & B_1 y^2 + c_1 y + c_2 + B_e^{-2k_n y} + B_3 e^{-2k_m y} \\ & + A_2 e^{-k_n y} [\sin(nt - k_n y) - \cos(nt - k_n y)] - A_3 e^{-2k_n y} \cos 2(nt - k_n y) \\ & - A_4 e^{-2k_m y} \cos 2(mt + \phi - k_m y) - A_2 e^{-\beta_1 y} \sin(nt - \beta_1 y) \\ & - A_2 e^{-\beta_1 t} \cos(nt - \beta_1 y) + A_3 e^{-\beta_2 y} \cos(2nt - \beta_2 y) \\ & + A_4 e^{-\beta_3 y} \cos(2mt + 2\phi - \beta_3 y) \end{aligned}$$

$$\beta_1 = \sqrt{\frac{n}{2} Pr \frac{\rho}{\mu}} \quad \beta_2 = \sqrt{n Pr \frac{\rho}{\mu}} \quad \beta_3 = \sqrt{m Pr \frac{\rho}{\mu}}$$

$$B_1 = -\frac{Pr c^2}{2C_p} \quad A_2 = \frac{2Ack_n}{C_p Re \left( n - \frac{2k_n^2 \mu}{\rho Pr} \right)}$$

$$B_2 = -A^2 \frac{Pr}{4C_p} \quad A_3 = \frac{A^2 k_n^2}{C_p Re \left( 2n - \frac{8k_n^2 \mu}{\rho Pr} \right)}$$

$$B_3 = -\beta^2 \frac{Pr}{4C_p} \quad A_4 = \frac{B^2 k_m^2}{C_p Re \left( 2m - \frac{8k_m^2 \mu}{\rho Pr} \right)}$$

$$C_1 = \frac{1}{y_e} \left[ T_{\infty} - C_2 + \frac{Pr c^2 y_e^2}{2C_p} \right]$$

$$C_2 = T_w + \frac{Pr(A^2 + B^2)}{4C_p}$$

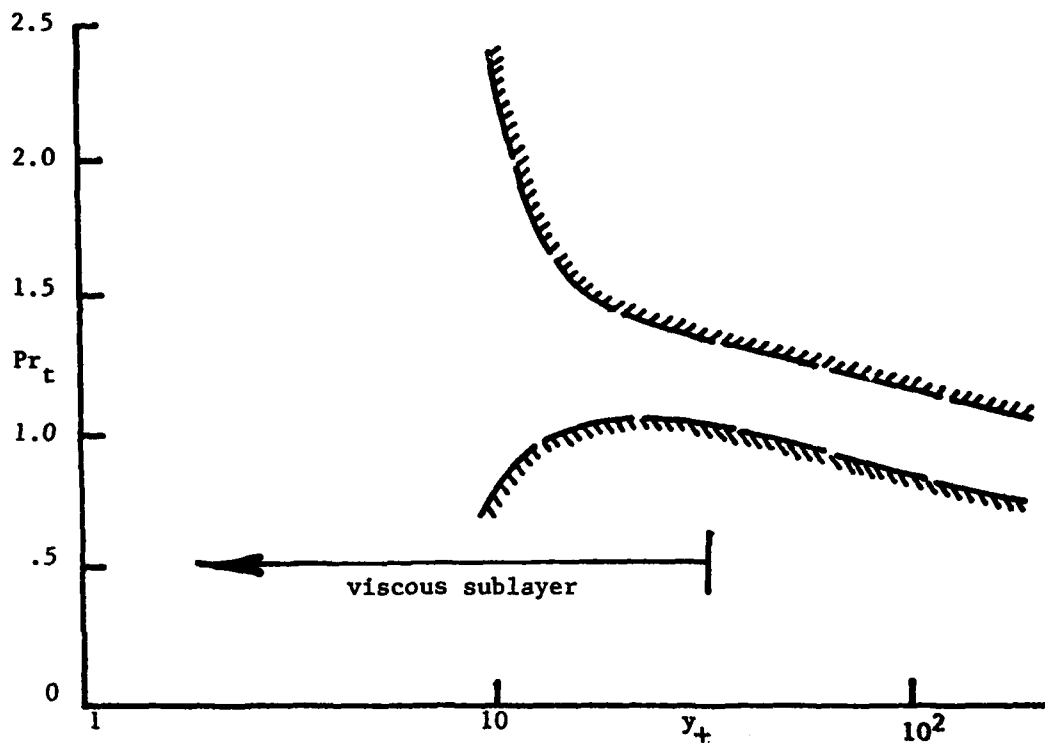


Figure 1. - Envelope of experimental uncertainty for turbulent Prandtl number from data of Simpson et. al. (1970).

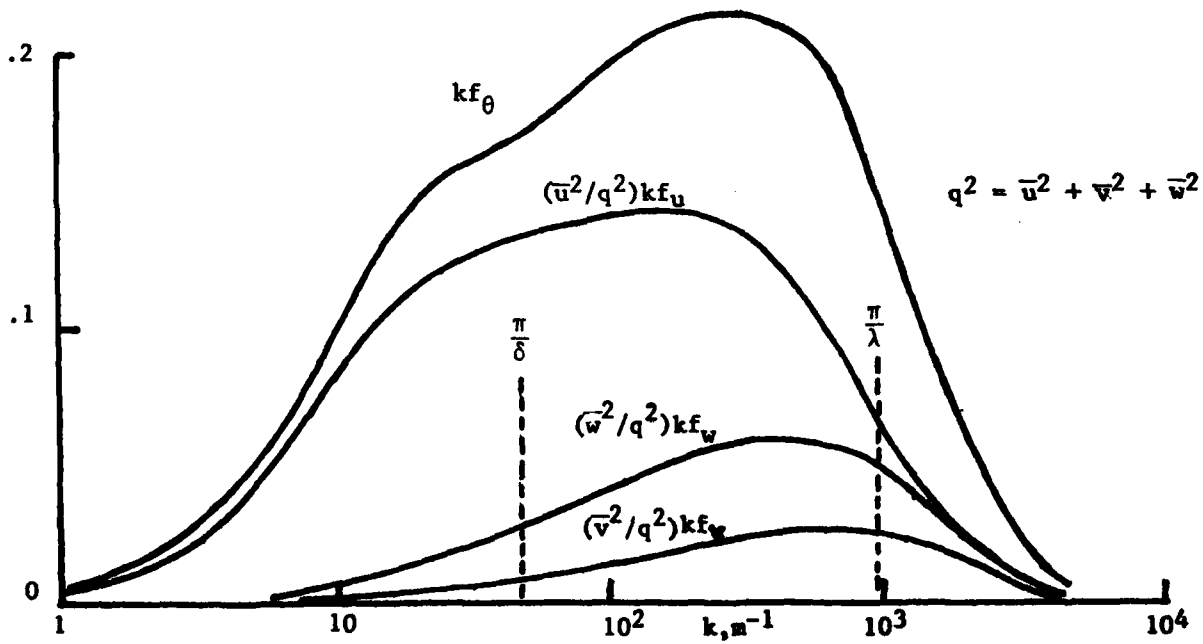


Figure 2. Spectral density of the three components of velocity fluctuation at  $y_+ = 40$  from data of Fulachier (1972).

# Theoretical Models for the Turbulent Pr

Molecular Pr = 0.720

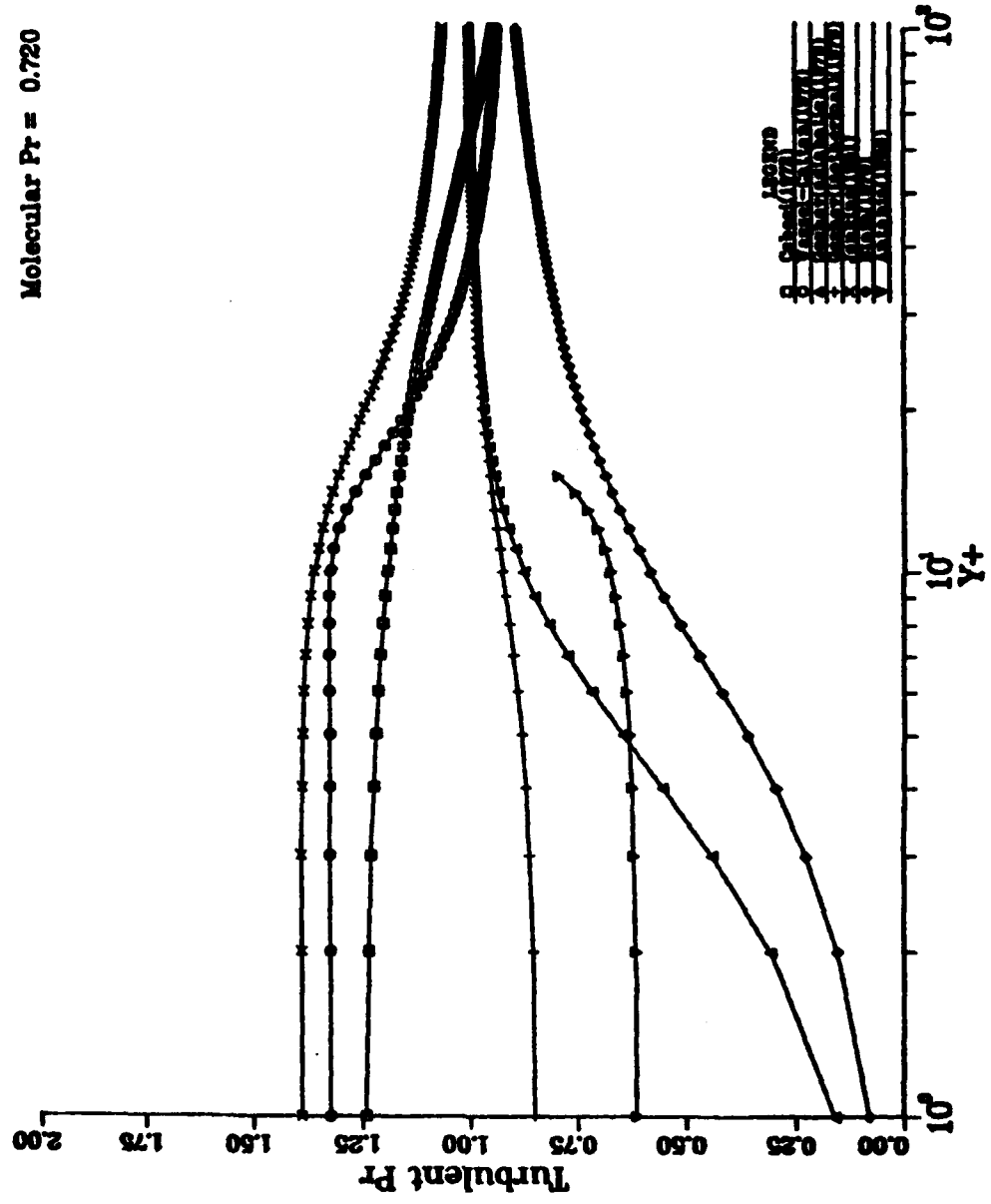


Figure 3. Some theoretical models of turbulent Prandtl number for a molecular Prandtl number of 0.72 (air).

# Theoretical Models for the Turbulent Pr

Molecular Pr = 6.000

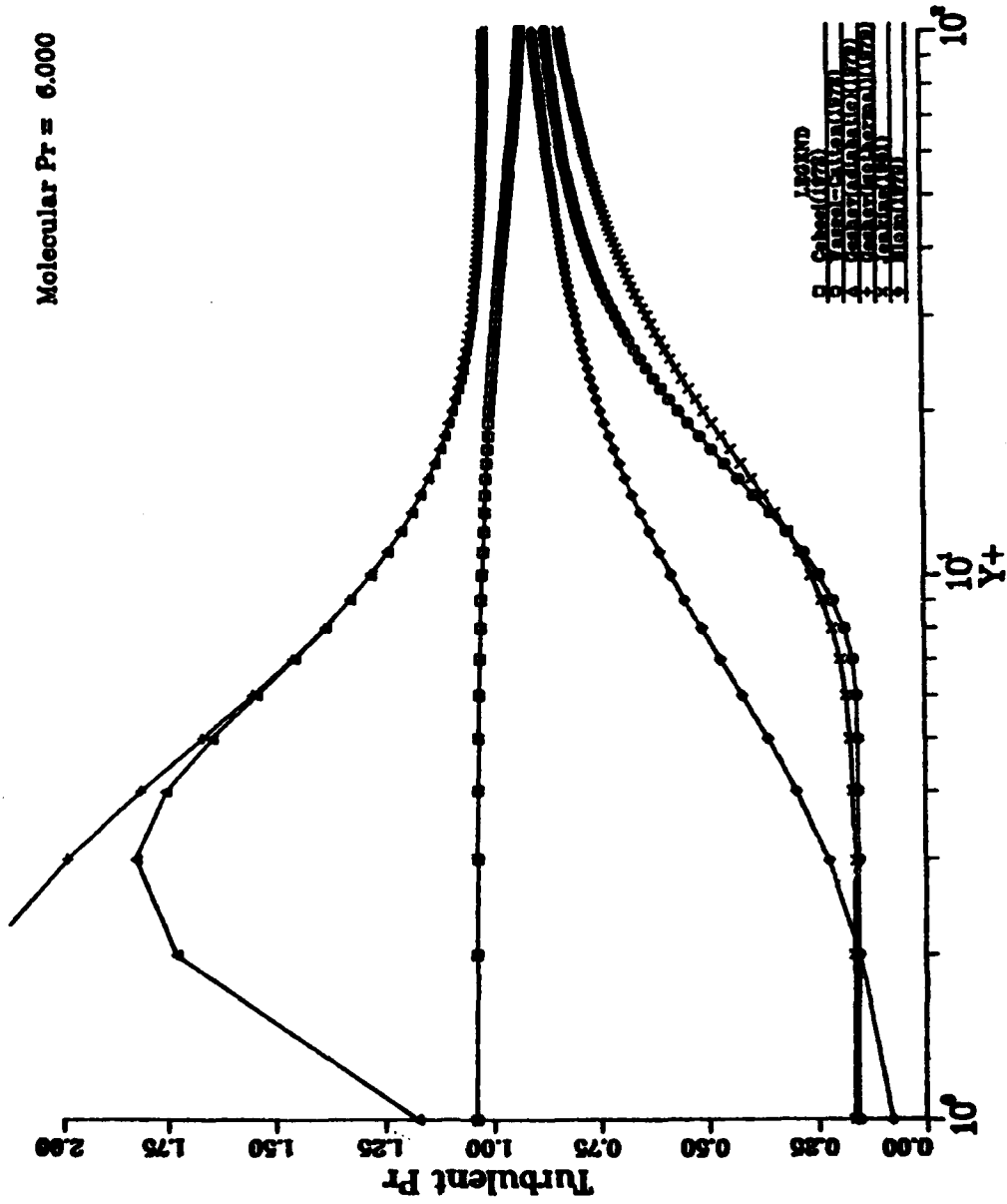
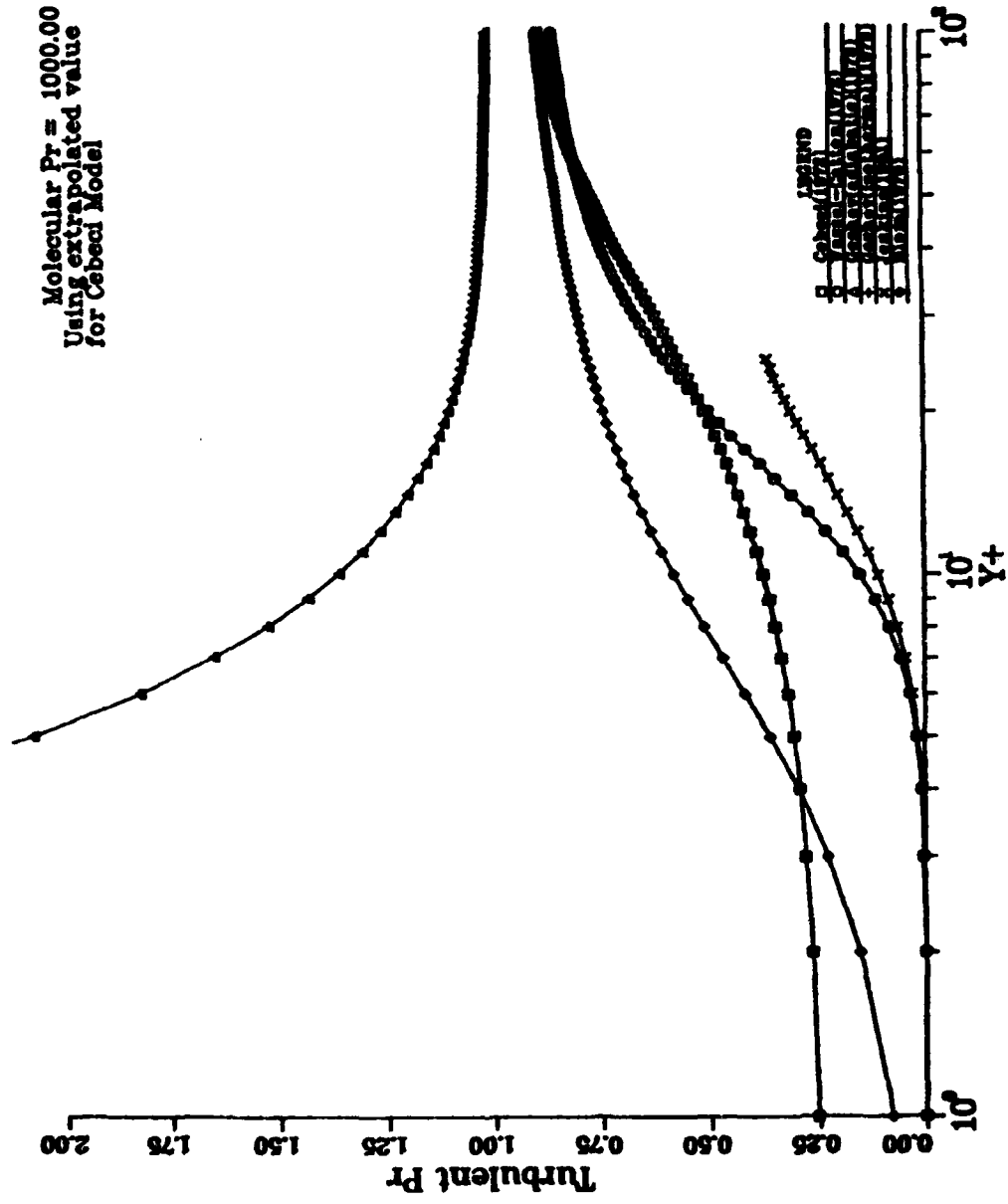


Figure 4. Some theoretical models of turbulent Prandtl number for a molecular Prandtl number of 6 (water).

# Theoretical Models for the Turbulent Pr



# CODE VERIFICATION

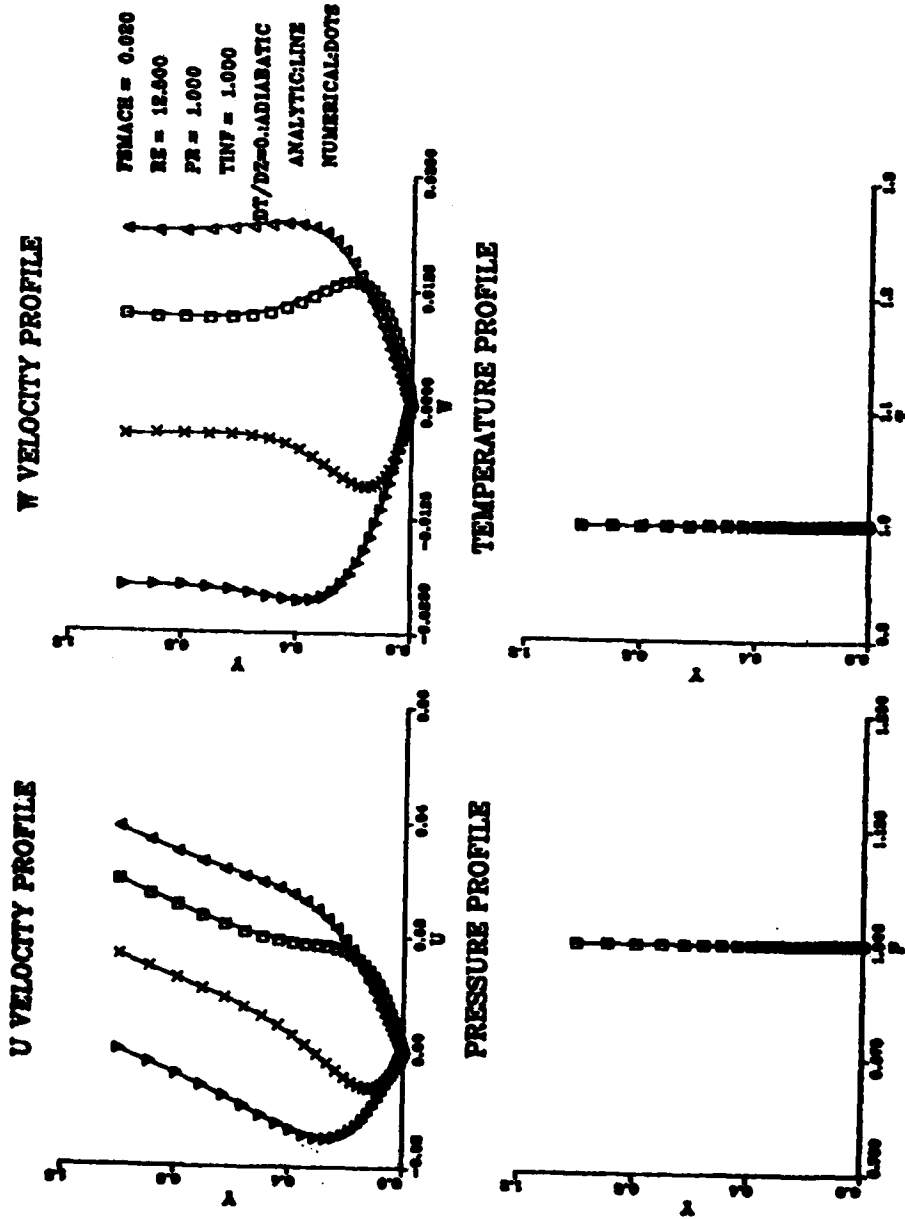


Figure 6. Comparison of numerical computations with exact analytical results for oscillating shear flow; Adiabatic wall.

# CODE VERIFICATION

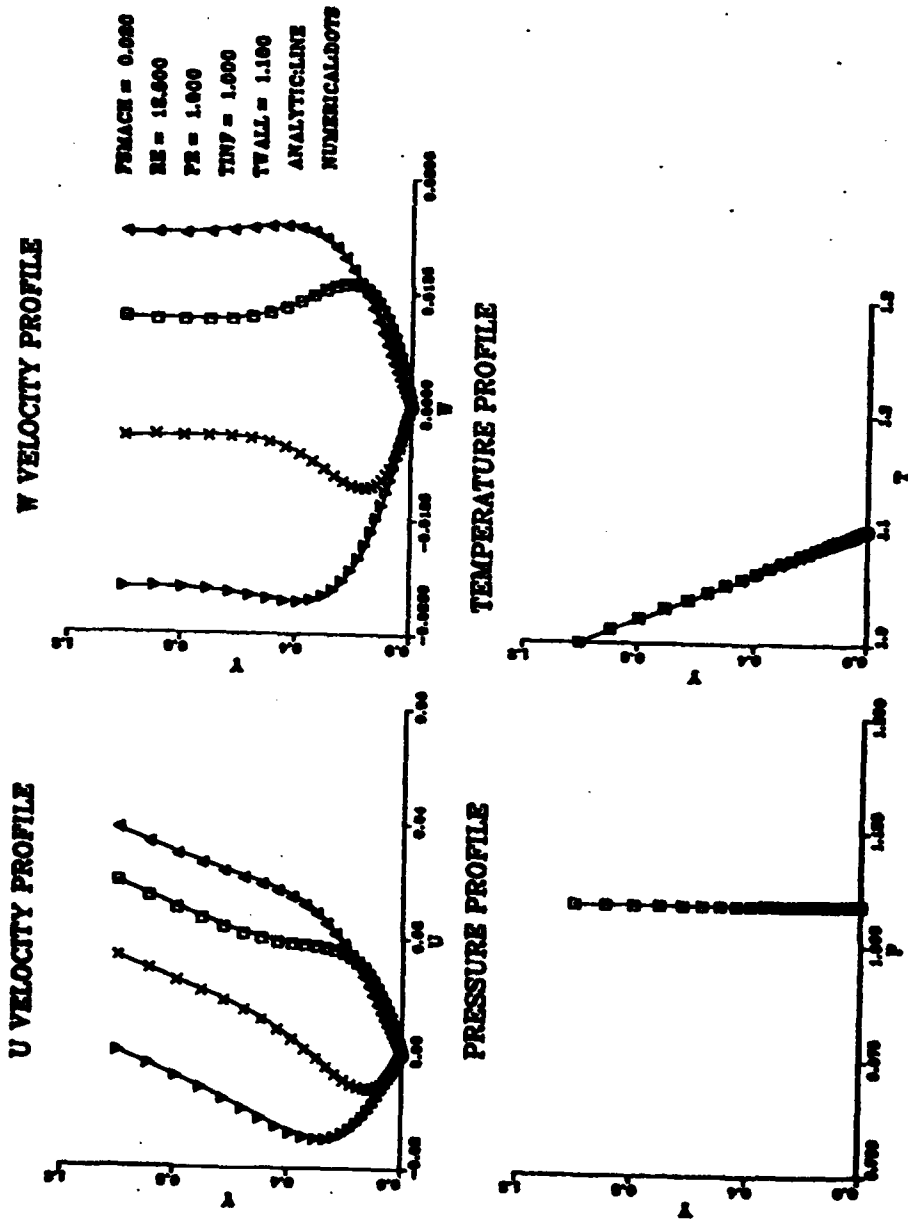


Figure 7. Comparison of numerical computations with exact analytical results for oscillating shear flow; Heat transfer case,  $T_w/T_\infty = 1.1$ .

DATE  
FILMED  
8